Visual and Quantitative Assessment of Poincaré Plots to Predict Mortality in Critically Ill Children

Jordan Walter Hutchinson

A thesis submitted to the faculty of the University of North Carolina at Chapel Hill in partial fulfillment of the requirements for the degree of Masters in Biomedical Engineering in The Department of Biomedical Engineering.

Chapel Hill
2013

Approved By:

Paul Dayton, PhD

Keith Kocis, MD, MS

Stephen Quint, PhD

Charles Schmitt, PhD

ABSTRACT

JORDAN WALTER HUTCHINSON: Visual and Quantitative Assessment of Poincaré Plots to Predict Mortality in Critically Ill Children
(Under the direction of Paul Dayton, PhD)

Heart rate variability (HRV) can be used as a noninvasive indicator of autonomic function.[1-4] Diminished or ectopic heart rate variability is associated with increased mortality in a variety of diseases in adult and pediatric patients.[5-9] Poincaré plots represent a non-linear method for visually displaying HRV. Poincaré plots are derived by graphing each normal RR interval (ms) against the subsequent RR interval. In healthy individuals, Poincaré plots take on a "Comet"-shaped pattern, which arises from the normal decrease in variability as heart rate slows.[10] In adults with advanced heart failure the plots are either "Torpedo" shaped, reflecting minimal variability within RR intervals; "Fan" shaped, reflecting diminished variability within RR intervals; or "Complex" shaped, reflecting random variability within RR intervals.[10] The present study aimed to determine whether resident physicians could predict whether critically ill children hospitalized in a Pediatric Intensive Care Unit (PICU) survived to discharge based on the interpretation of Poincaré plots.

ACKNOWLEDGEMENTS

Dr. Paul Dayton for guidance and role of a mentor.

Dr. Keith Kocis, Dr. Stephen Quint, and Dr. Charles Schmitt: whose wealth of knowledge provided very helpful advice, direction, and support for this work.

My family and friends for the constant support and encouragement.

TABLE OF CONTENTS

LIST OF TABLES

LIST OF FIGURES

LIST OF ABBREVIATIONS

AMI	Acute Myocardial Infarction
ANS	Autonomic Nervous System
BP	Blood Pressure
BPM	Beats per Minute
CD	Cumulative Distance
CHF	Congestive Heart Failure
ECG	Electrocardiogram
FHR	Fetal Heart Rate
HF	High Frequency
HR	Heart Rate
HRV	Heart Rate Variability
LF	Low Frequency
MAD	Median Absolute Deviation
ms	Milliseconds
NN	Intervals between normal (sinus) beats
NPV	Negative Predictive Value
PICU	Pediatric Intensive Care Unit
PPV	Positive Predictive Value
PSNS	Parasympathetic Nervous System

RR	R wave to R wave
SD	Standard Deviation
SDNN	Standard Deviation of NN Interval
SNS	Sympathetic Nervous System
ULF	Ultra Low Frequency
VLF	Very Low Frequency

CHAPTER 1

INTRODUCTION

The measurement of Heart Rate Variability (HRV) is a valuable tool in both clinical practice and physiological research. The problem herein is predicting mortality during hospitalization from heart rate variability metrics and from the visualization of such metrics. Many patients come through the doors, and some of the questions that arise during hospitalization are: “Who needs immediate attention to prevent hospital mortality?”, “How should valuable resources (human (MD, RN) and physical locations (ICU beds)), be divided and triaged?”, and “How can families be counseled during the course of hospitalization?”

HRV is the measurement of beat-to-beat fluctuation in the heart rate. HRV is a normal physiologic mechanism, which is sometimes referred to as sinus arrhythmia. HRV reflects the dynamic response of cardiovascular control systems to physiologic perturbations such as respiration and thermoregulation.

Sinus arrhythmia refers to a normal phenomenon of mild acceleration and slowing of the heart rate that occurs with breathing. It is usually quite pronounced in children and steadily decreases with age. HRV can also be present during meditation breathing exercises that involve deep inhaling and breath holding patterns.[11-12] Acute life threatening and chronic illness may also impact normal heart rate variability.[1-3,13-15]

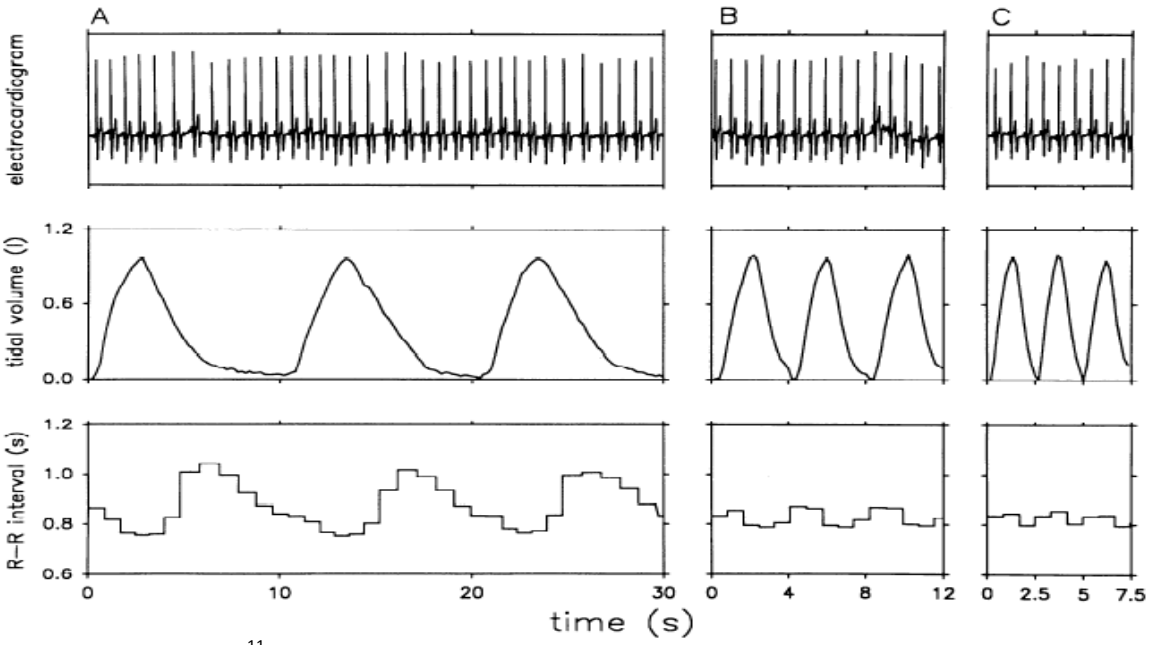

Figure 1. Brown[11]. Experimental records from 1 subject. Respiratory rates shown are 6 (A), 15 (B), and 24 breaths/min (C). RR interval variability is greatest at slowest breathing rate.

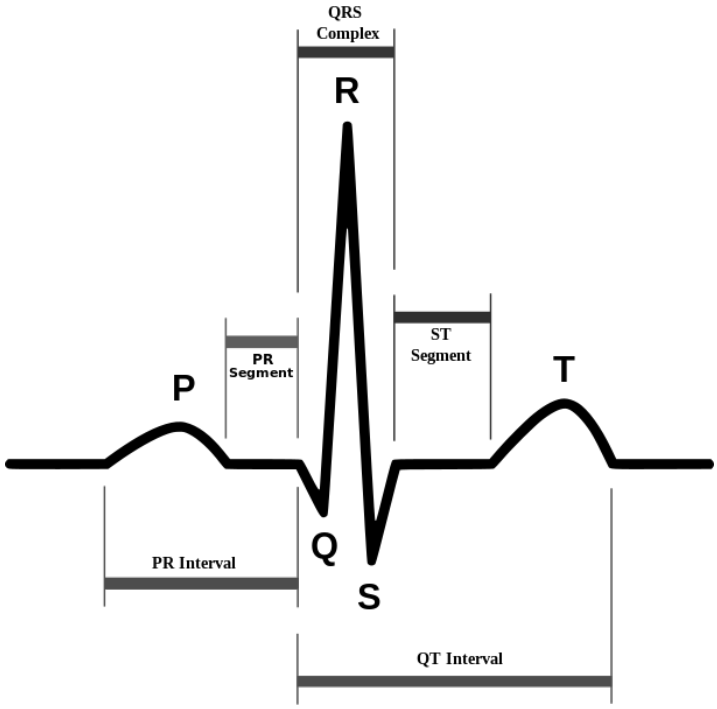

Figure 2. Graphical representation of the different intervals obtained in a normal electrocardiogram.

The RR interval is the interval from the peak of the R wave in one QRS complex, as shown in Figure 2, to the peak of the next R wave. The QRS complex is used to measure the ventricular rate by taking 60 and dividing by the RR interval (measured in seconds). The term NN is used in place of RR to emphasize the fact that the processed

beats are "normal" beats. HRV is measured using the NN interval and provides a noninvasive indicator of autonomic nervous system tone.[10] Under normal conditions, heart rate increases with inspiration (decreased intra-thoracic pressure, increased venous return → increased sympathetic nervous system (SNS) tone → increased heart rate), and decreases with expiration (increased intra-thoracic pressure, decreased venous return → increased parasympathetic nervous system (PSNS) tone →decreased heart rate). Beat-to-beat changes in blood pressure (BP) are due to various physiologic mechanisms regulated by the autonomic nervous system (ANS: SNS & PSNS). HRV is the efferent limb; it is (part of) the response of the ANS to keep BP stable. The effect of the ANS output works very quickly (on the order of milliseconds.)

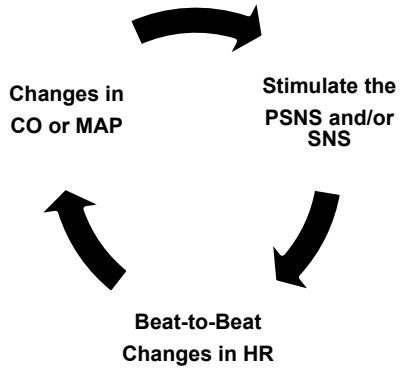

Figure 3. Homeostatic regulation of Heart Rate (HR)

As discussed, HRV is normal and healthy and reduced HRV is pathological. The loss of HRV is reported to reflect an alteration in autonomic nervous system function. A number of disease states are associated with changes in HRV, including heart failure, sudden infant death syndrome, myocardial infarction, prematurity, neonatal respiratory distress syndrome, and diabetes to name a few.[1-4,13-15]

Fetal Heart Rate (FHR) monitoring was one of the first areas in which this phenomenon was recognized and important clinical observation and intervention begun.[16] It was discovered that abnormal heart rate variability during and after uterine contraction indicated fetal distress and is used as an indication for immediate caesarean

section delivery. The diminution of the beat-to-beat variation in the fetal HR during labor signifies fetal distress and the need for rapid delivery.[1]

In 1987, Kleiger[6] obtained 24 hours of continuous Electrocardiogram (ECG) data recorded 11 ± 3 days after Acute Myocardial Infarction (AMI) and analyzed the data for HRV. The mortality is 5.3 times higher in patients with a standard deviation (SD or SDNN) of HRV less than 50 milliseconds (ms) versus patients with SD of HRV greater than 100ms. A hypothesis for explaining the results infers that low PSNS and high SNS is abnormal and potentially predisposes patients post AMI to ventricular fibrillation.

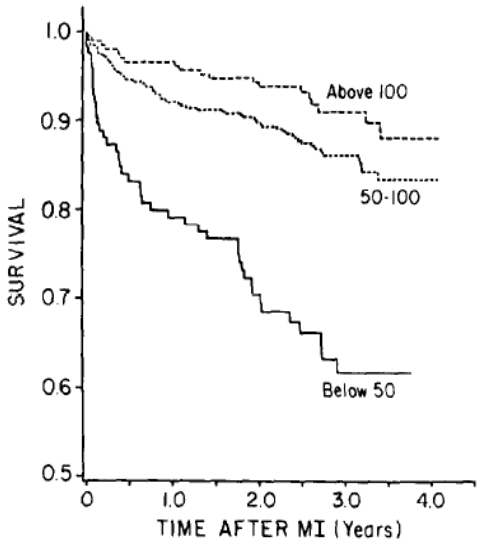

Figure 4. Cumulative survival over total follow up period as a function of HRV. Survival curves are calculated by the method of Kaplan & Meier.[17]

Kleiger uses the standard deviation of RR intervals (ms) metric to quantify HRV. With a SD less than 50ms, equating to low variability (RR interval is nearly the same length every beat), the total mortality during 31 month follow up is 34.4% (odds ratio of 5.3). With a SD of 50-100ms (moderate HRV), the total mortality during follow up is 13.8% (odds ratio of 1.6). Lastly, if the SD is greater than 100ms (good HRV), the total mortality during follow up is 9.0% (odds ratio of 1.0). The conclusion of the study shows that the lack of HRV predicts long-term mortality after acute myocardial infarction. Poincaré plots to analyze HRV have not been previously applied in the PICU setting.

HRV is often measured by the standard deviation (SD) of the RR intervals over a given time interval. In doing so, beat-to-beat temporal information is lost to retain a metric on overall temporal fluctuation. A larger SD equates to more HRV and a smaller SD equates to less HRV. Just as there are time domain measures of HRV, there exist frequency domain measures of HRV. Current HRV analysis contains a family of metrics; time domain, including SD, Frequency domain, as well as non-linear metrics.

Variable	**Units**	**Description**
		Statistical Measures
SDNN	ms	Standard Deviation of all NN intervals.
SDANN	ms	Standard Deviation of the averages of NN intervals in all 5-minute segments of the entire recording.
RMSSD	ms	The square root of the mean of the sum of the squares of differences between adjacent NN intervals.
SDNN INDEX	ms	Mean of the Standard Deviations of all NN intervals for all 5-minute segments of the entire recording.
SDSSD	ms	Standard Deviation of the differences between adjacent NN intervals.
NN50 count		Number of pairs of adjacent NN intervals differing by more than 50ms in the entire recording; three variants are possible counting all such NN intervals: pairs or only pairs in which the first or the second interval is longer.
pNN50	%	NN50 count divided by the total number of NN intervals.
		Geometric Measures
HRV Triangular Index		Total number of all NN intervals divided by the height of the histogram of all NN intervals measured on a discrete scale with bins of 7.8125ms (1/128 seconds).
TINN	ms	Baseline width of the minimum square difference triangular interpolation of the highest peak of the histogram of all NN intervals.
Differential Index	ms	Difference between the widths of the histogram of differences between adjacent NN intervals measured at selected heights (e.g. At the levels of 1000 and 10000 samples).
Logarithmic Index		Coefficient φ of the negative exponential curve $ke^{-\varphi t}$, which is the best approximation of the histogram of absolute differences between adjacent NN intervals.

Table 1. Task Force[18]. Selected time domain measures for assessing HRV.

Variable	Units	Description	Frequency Range
Analysis of Short-term Recordings (5 min)			
5-min total power	ms^2	The variance of NN intervals over the temporal segment	~≤0.4 Hz
VLF	ms^2	Power in the VLF range	≤0.04 Hz
LF	ms^2	Power in the LF range	0.04-0.15 Hz
LF norm	nu	LF power in normalized units LF/(total power – VLF)x100	
HF	ms^2	Power in HF range	0.15-0.4 Hz
HF norm	nu	Power in normalized units HF/(total power – VLF)x100	
LF/HF		Ration LF(ms^2)/HF(ms^2)	
Analysis of Entire 24 Hours			
Total power	ms^2	Variance of all NN intervals	~≤0.4 Hz
ULF	ms^2	Power in the ULF range	≤0.003 Hz
VLF	ms^2	Power in the VLF range	0.003-0.04 Hz
LF	ms^2	Power in the LF range	0.04-0.15 Hz
HF	ms^2	Power in the HF range	0.015-0.4 Hz
α		Slope of the linear interpolation of the spectrum in a log-log scale	~≤0.4 Hz

Table 2. Task Force[18]. Selected frequency domain measures for assessing HRV.

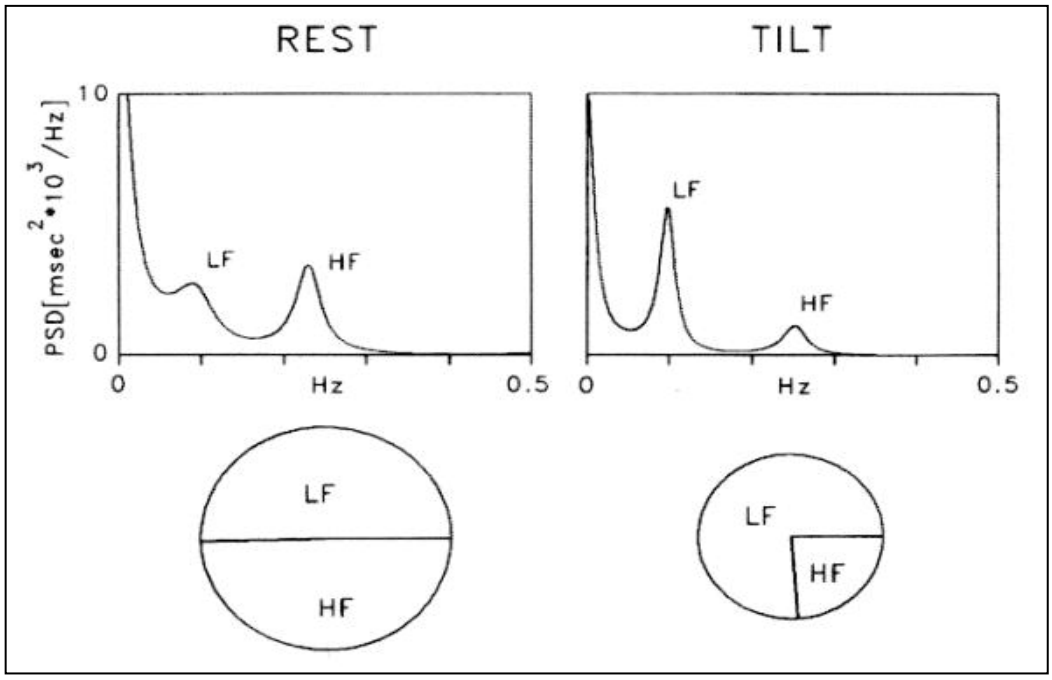

Figure 5. Spectral analysis (autoregressive model, order 12) of RR interval variability in a healthy subject at rest and during 90 degrees head-up tilt.

Variable	Units	Normal Values (mean ± SD)
Time Domain Analysis of Nominal 24 hours		
SDNN	ms	141 ± 39
SDANN	ms	127 ± 35
RMSSD	ms	27 ± 12
HRV Triangular Index	ms	37 ± 15
Spectral Analysis of Stationary Supine 5-min Recording		
Total Power	ms^2	3466 ± 1018
LF	ms^2	1170 ± 416
HF	ms^2	975 ± 203
LF	nu	54 ± 4
HF	nu	29 ± 3
LF/HF ratio		1.5-2.0

Table 3. Task Force[18]. Normal values of standard measures for assessing HRV.

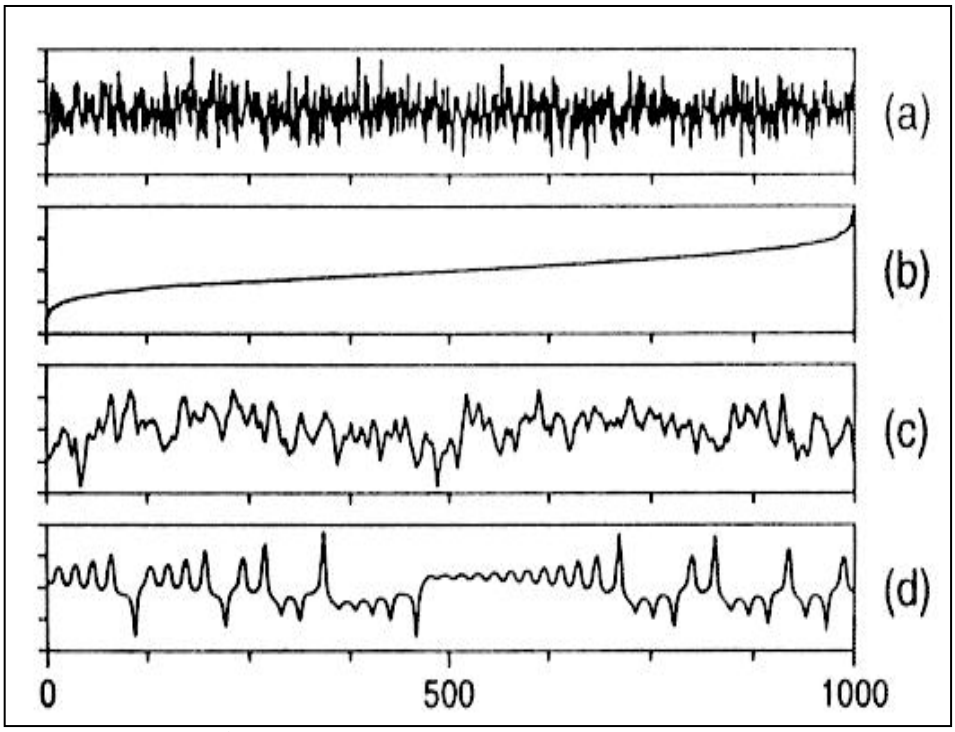

Figure 6. Kaplan[19]. Example of four synthesized time series with identical means, standard deviations, and ranges. Series (c) and (d) also have identical autocorrelation functions and therefore identical power spectra.

The predominant problem with using summary statistics (used to summarize a set of observations, in order to communicate the largest amount of knowledge as efficiently as possible) in medicine is that the loss of information can obscure data patterns that may otherwise better inform care decisions. As seen in Figure 6 above, using the summary statistics of mean, standard deviation, and range will result in the same conclusion

regardless of the waveform pattern. Many patients with heart failure have arrhythmias that make the raw heart rate variability data less suitable for the use of summary statistical measures. This is the issue of RR (which may be an abnormal ectopic beat) vs. the NN (which is the normal sinus beat) – each is handled in a different way. Non-linear methods may be better suited to extracting salient information contained within physiological waveforms.

In 1992, Woo[10] et al introduced the use of Poincaré plots as a novel method for analyzing HRV. Poincaré plots have the benefit of presenting a summarized view of EKG data while preserving evolving visual patterns in EKG data, thus suggesting their usefulness in medical decision support.

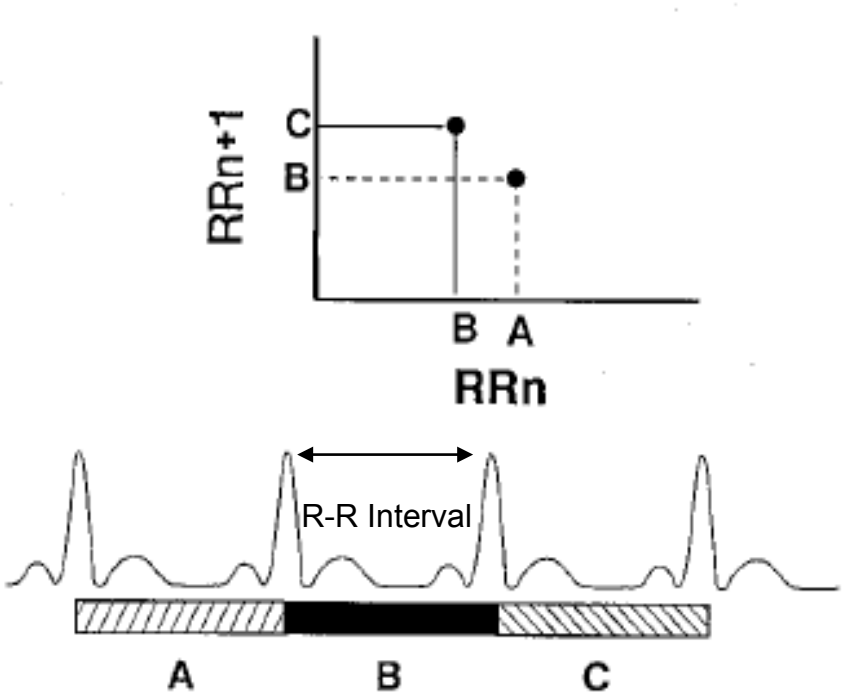

Figure 7. Woo[10]. Construction of Poincaré plot from ECG wave. A, B, and C represent consecutive RR intervals.

As shown in Figure 7, Poincaré Plots can be plotted on a Cartesian plane from RR interval data. The first point is created using the A interval as the x-coordinate and interval B as the Y-coordinate. The second point uses the B interval as the x-coordinate and the C interval as the y-coordinate. The remaining points are constructed using each interval in turn as first the x-coordinate and then, in the next point, as the y-coordinate.

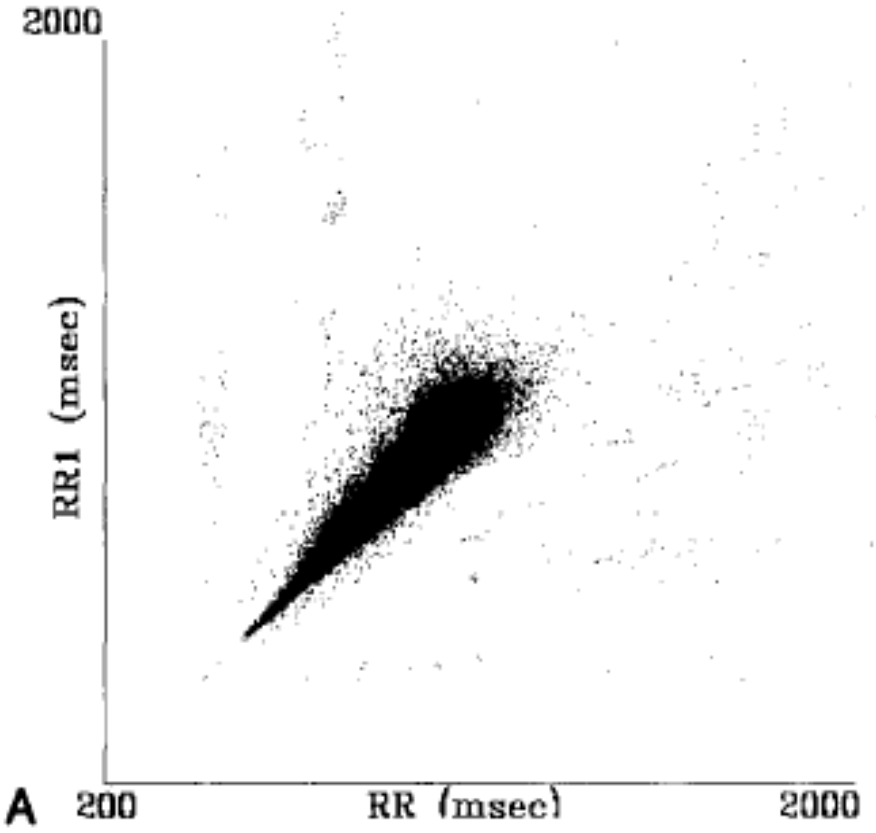

Figure 8. Woo[10]. This "Comet" shape (shown above) is normal for 24 hour recordings, other shapes are not.

Woo showed Comet patterns, as seen Figure 8, representing healthy patients, and other 3 shapes (see Figure 9), seen in pathologic states such as congestive heart failure (CHF) patients. Decreased HRV is associated with an increased mortality rate in CHF patients. Woo demonstrated Poincaré plots in twenty-four CHF patients and compares this to twenty-four healthy controls. All health controls had a Comet shape pattern to their Poincaré plot. No patients with CHF had the Comet shape, yet findings show there was no statistical significance in predicting sudden death.

The Comet pattern (Figure 9A) demonstrates a wide range of RR intervals, typically extending from 500-1000ms (equivalent to heart rates of 120-60 BPM, respectively) along both axes. Also, as the RR interval increases (i.e. slower heart rates), the dispersion of subsequent intervals increases. As HR slows, the inter-beat variation

increases, creating the distinctive Comet pattern. As the RR intervals lengthen on the x-axis, the next RR interval (plotted on the y-axis) is more variable, seen as the widening of the tail of the Comet. Shorter RR intervals equal faster HRs and there is less HRV, (i.e. the length of RR interval does not vary as much between beats). Thus, the head of the Comet is narrower.

As seen in Figure 9B, the Torpedo pattern reflects low RR interval dispersion over the range of HR; regardless of HR, there is low variability at both slower and faster HRs. The Fan pattern (Figure 9C) reflects restriction in the range of RR intervals with enhanced variability seen (i.e. dispersion). The Complex pattern (Figure 9D) shows clusters of points characteristic of erratic changes in RR intervals, consistent with non-linear behavior. This indicates jumps in HR from beat to beat, with long RR-intervals being juxtaposed to short RR-intervals. It should be noted that the mechanisms of these different patterns are not understood and are thus a rich area for future investigations.

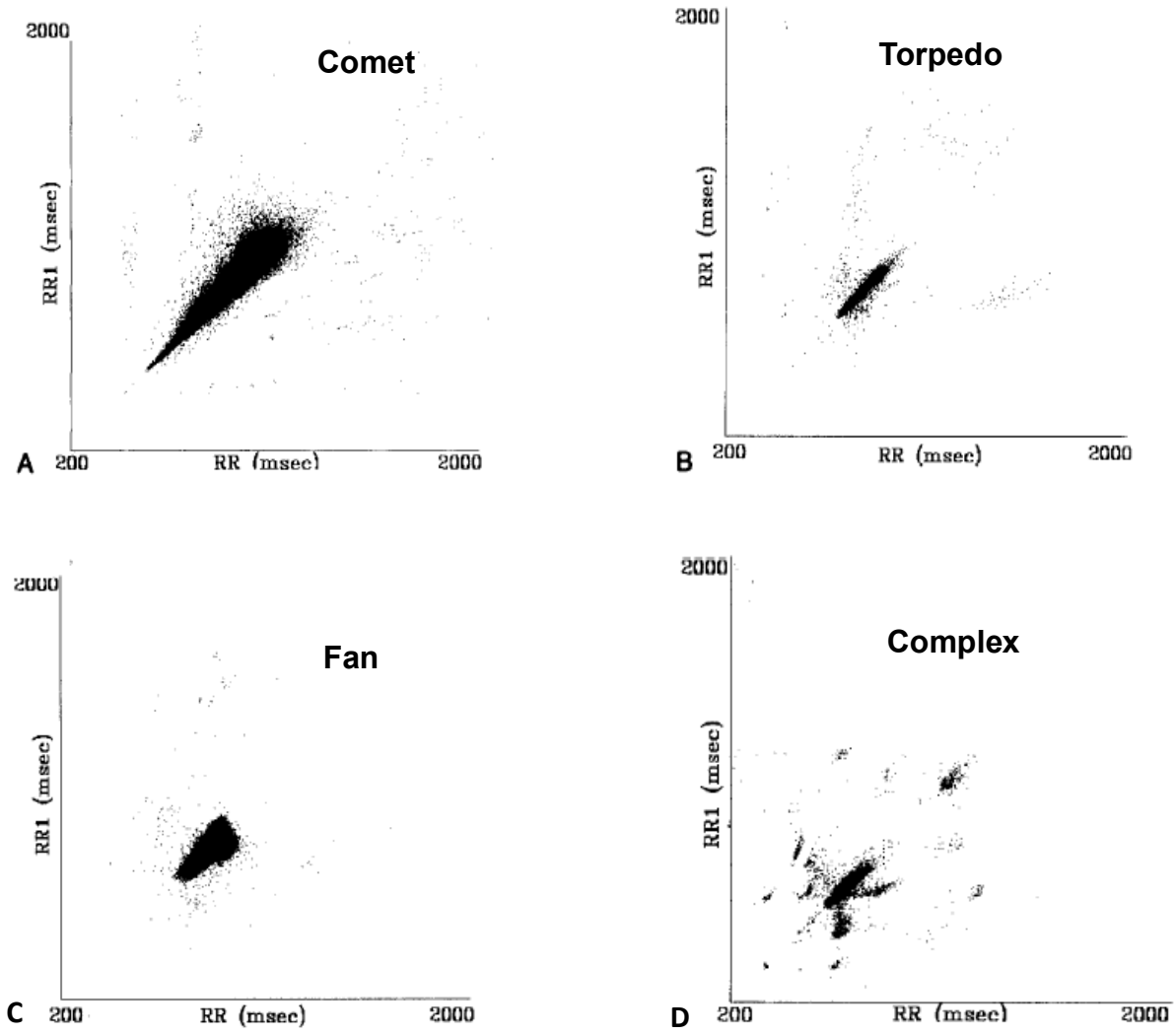

Figure 9. Woo[10]. The four predominant shapes described as (A) Comet, (B) Torpedo, (C) Fan, and (D) Complex.

Poincaré patterns could not be directly predicted from the SD of RR intervals, thus different information is provided through the use of the Poincaré method. Benefits of using the Poincaré method for plotting HRV include:

1. Simultaneous display of overall variance, dispersion of RR intervals at HR, and change in variance at cardiac rate changes[10]
2. Ease of visual assessment
3. Nonlinear processing is more readily deciphered by the human brain

4. Assessment of instantaneous variation at different HRs

5. Outlier (ectopic beat or artifact) identifier

The Comet pattern, seen in all healthy volunteers, differed markedly from the other three patterns exhibited exclusively by the CHF patients. Diminished HRV is associated with high sympathetic tone and an increased mortality rate in CHF patients. Inter-observer agreement (Kappa) between four blinded observers was 96% (23/24 patients). Items such as physical exam findings, radiographic interpretations, or other diagnostic tests often rely on some degree of subjective interpretation by observers. Studies that measure the agreement between two or more observers should include a statistic that takes into account the fact that observers will sometimes agree or disagree simply by chance. The Kappa statistic (or Kappa coefficient) is the most commonly used statistic for this purpose. It gives a score of how much homogeneity, or consensus, there is in the ratings given by judges. It is useful in refining the tools given to human judges, for example by determining if a particular scale is appropriate for measuring a particular variable. If the ratings between the individuals do not agree, then either the scale is defective or the rating individuals need to be re-trained.

To date, studies have tried to extract summary statistics from Poincaré plots with limited success to explain the data differently than time domain and frequency domain methods. Brennan[20] aimed to determine if summary descriptors based on Poincaré plots are independent of existing HRV measures. Tulppo[21] created an ellipse fitting technique to the Poincaré plot in order to describe its shape. From the ellipse, a set of axes oriented with the line of identity is defined as:

1. SD1 – Perpendicular to the line of identity; shows short-term variability.

2. SD2 – Collinear to the line of identity; shows long-term variability.

It is often suggested[22-30] that indices can be derived from Poincaré plots that are able to measure quantities of the variability that are nonlinear and or independent of the standard linear indices, but Brennan[20] shows that this is not the case. No measure derived from Poincaré plots to date have been shown to be independent of standard

linear time domain or frequency domain measures of HRV. Therefore, the intrinsic ability of the Poincaré plot to identify nonlinear beat-to-beat structure is not being exploited quantitatively.

CHAPTER 2

STUDY METHODS

AIM 1. The first aim of the study was to evaluate the use of Poincaré plots, visual displays of heart rate variability, to predict mortality in critically ill children admitted to the pediatric intensive care unit (PICU).

Twelve subjects who died in the Pediatric Intensive Care Unit (PICU) were compared against twelve age-matched subjects who survived to discharge from the PICU. Poincaré plots were generated using continuous ECG data streams from all twenty-four subjects. ECG data streams from Spacelabs (CA, USA) critical care patient monitors were obtained at 896 Hz but decimated by the manufacturer to 225 Hz for storage. These were then filtered for noise and then the R peak was automatically identified (fiducial point) through a series of biomedical engineering algorithms, and stored in a back-end archival database.

The data was extracted from the database file of fiducial points listed in Coordinated Universal Time (UTC) of occurrence. From each R peak time indication, differences were calculated to determine the RR interval. Once tabulated, ectopic beats and noise were eliminated from the data by restricting the BPM range to 40 – 250.[31] The Poincaré plots were generated over thirty minute epochs during the patient stay in the PICU and displayed in a movie format, with each subsequent plot changing every five seconds.

Two physician anesthesia resident reviewers were trained, blinded to patient outcome, and independently analyzed the plots for interpretation of the different shapes present in the Poincaré plots. The residents reviewed the plots for instances of Comet, Torpedo, Fan, and Complex shapes. The residents reviewed the entire movie of each patient, which were of different durations depending on the length of stay of the particular patient. The residents were trained to assess the predominant shape (of highest occurrence) for each thirty minute epoch in the movie in order to make the predictions, which were then compared to actual patient outcomes to assess the ability

of Poincaré plots to predict patient mortality. The data analysis procedure is summarized in Figure 10.

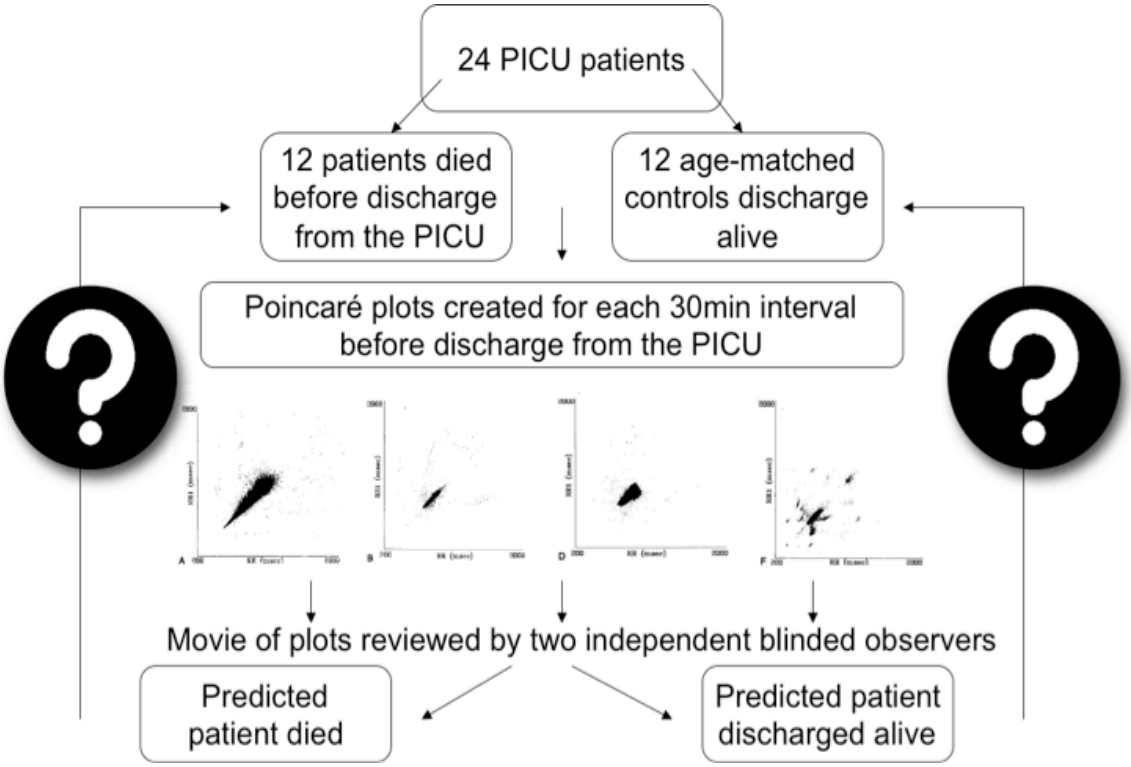

Figure 10. Graphical representation of study protocol.

AIM 2. The second aim of the study was to evaluate the use of cluster analysis on the Poincaré plots generated in order to automate predictions in patient outcome with high confidence. Automation also removes subjective biases introduced by individuals making the predictions.

K-means clustering is an unsupervised learning algorithm that aims to partition the *n* observations into k sets so as to minimize the within-cluster sum of squares. The algorithm for minimizing the sum of squares is per the criterion

$$J = \underset{S}{\arg\min} \sum_{j=1}^{k} \sum_{n \in S_j} |x_n - \mu_j|^2 , \quad (1)$$

where x_n is a vector representing the n^{th} data point and μ_j is the geometric centroid , using Euclidean distance, of the data points in S_j. For step 1, the centroid is computed for each set. In step 2, every point is assigned to the cluster whose centroid is closest to that point. The resultant clusters indicate geometric centers of mass, or locations showing where groups of data lie. K-means clustering was implemented here with 9 centers ($k = 9 \leq n$; n = each datum in a 30 minute epoch ≈ 2000 heartbeats).

K-means clustering has been used extensively in medical imaging.[32-37] The two key features of *k*-means which make it efficient are often regarded as its biggest drawbacks:

1. The number of clusters *k* is an input parameter: an inappropriate choice of *k* may yield poor results. For this data, 9 centers were heuristically determined to be appropriate.
2. Convergence to a local minimum may produce counterintuitive (wrong) results. For this data, local minimums do not affect the results because the analyses account for local minimums.[38]

The 9 data clusters (J_1, J_2, …, J_9) are characterized with number of data points belonging per cluster as well as the locations of each. From this information, one qualitative map is created and two statistics are calculated, where the focus is on

characterization of the dispersion of points (a large deviation is used as an indicator for death), with the hypothesis that as HRV deviates largely from HRV of healthy individuals, survivability decreases.[17,39] The two statistics are:

1. Cumulative Distance (CD) from ideal centers – How severely different is the current 30 minute epoch Poincaré pattern from the ideal Poincaré pattern?

   The Cumulative distance from ideal centers is calculated as

$$CD = \sum_{n=1}^{9} \left(\sqrt{x_{\mathrm{n}} - y_{\mathrm{n}}}\right)^2, \quad (2)$$

, (2)

   where x_{n} is a vector representing the n^{th} computed center location and y_{n} is a vector representing the n^{th} ideal center location.

2. Median Absolute Deviation (MAD) – a robust measure of the variability of a univariate sample of quantitative data and defined as the median of the absolute deviations from the data's median.

   The MAD is calculated as

$$MAD = median(|x - median(x)|), \quad (3)$$

   where x is an array of RR intervals over a thirty-minute epoch.

For the cumulative distance from the ideal centers statistic, the first step was to create centers that exemplify the Comet shape. Since the Comet shape is the reference shape seen in healthy individuals, it is used herein for comparison. For each thirty-minute epoch generated for a patient, the resultant plot will be compared against the reference Comet plot.

Using Matlab® (R2009a, The Mathworks, Natick, MA), ideal center locations are created in the process of first creating a random Gaussian distribution of 100,000 data points within the x-y square plane defined by the minimum (40) and maximum (250)

beats per minute of the Poincaré plot. Once created, the outline of the Comet shape was traced to indicate which of those points are to be saved, as seen in Figure 11.

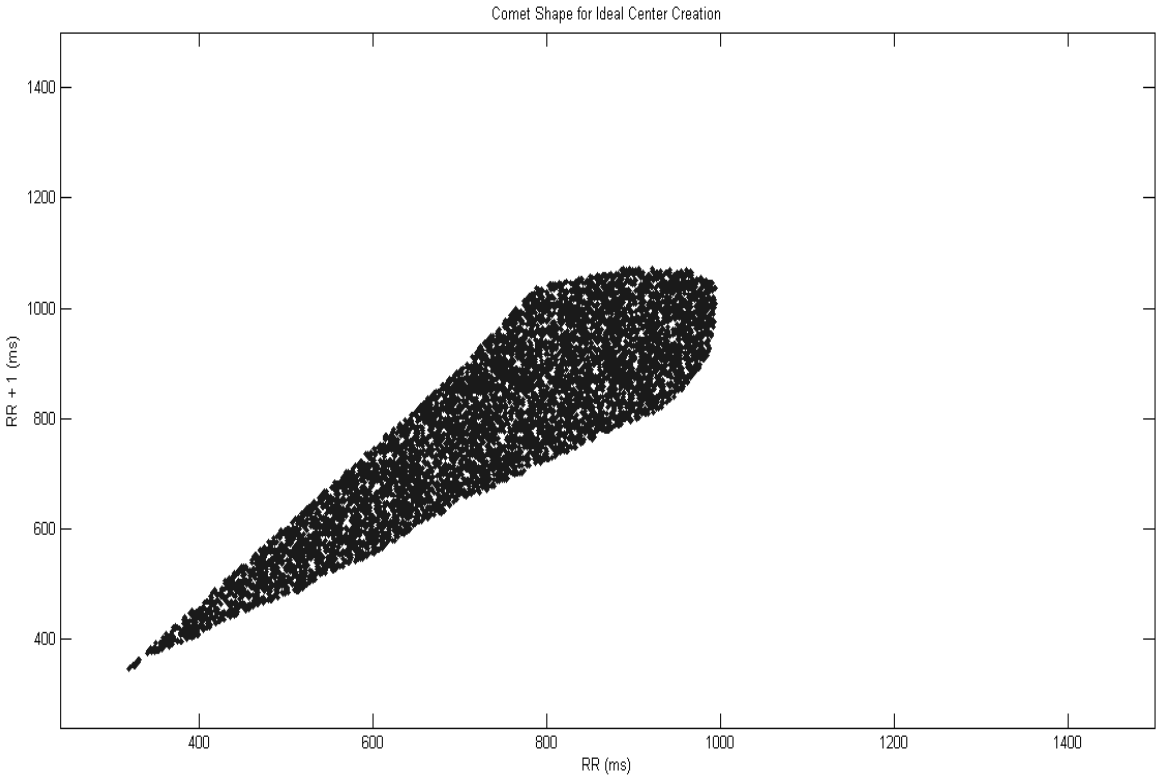

Figure 11. Resultant ideal Comet shape of data points for cluster analyses.

The saved points of Figure 11 were put through the same 9-center *K*-means cluster processing analysis as defined in Aim 1, resulting in the graph of geometric centers shown in Figure 12. Figure 13 shows a plot of the ideal centers with the centers created for the first thirty-minute epoch for patient 1 superimposed. For each thirty-minute epoch, distances are calculated for each center that is projected onto the associated ideal center. The distances are then summed to provide the summary statistic for the given epoch.

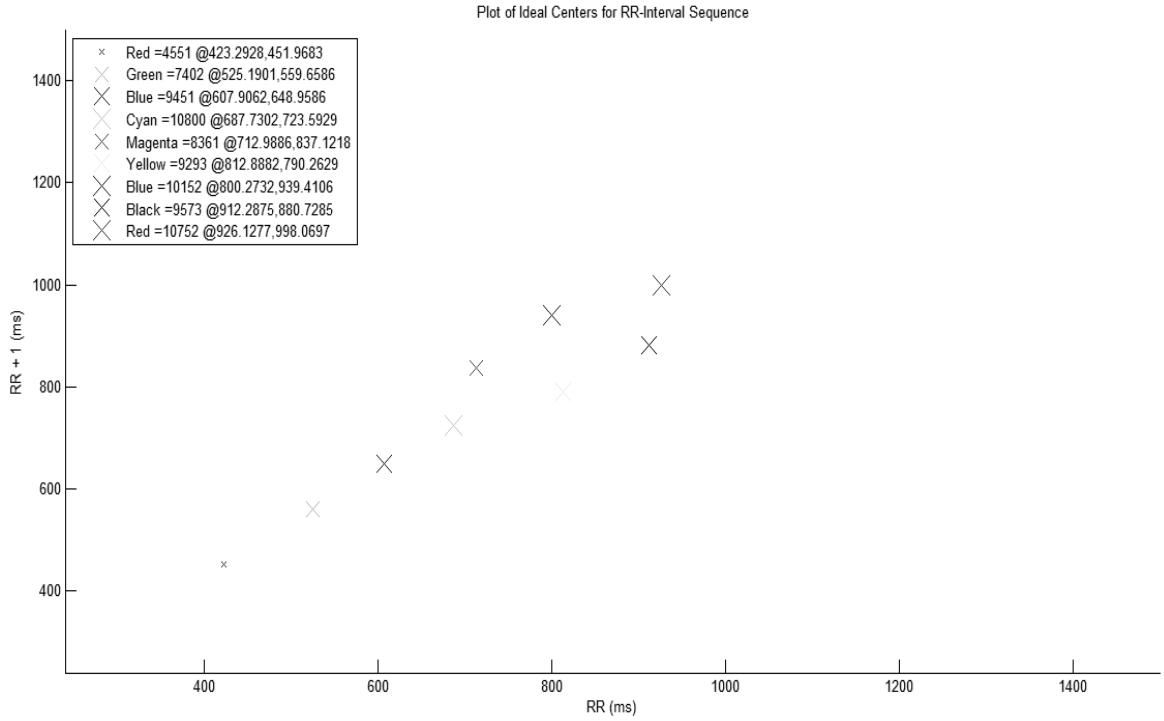

Figure 12. Graph of reference ideal centers with relative magnitude (number of datapoints associated with each center) and locations displayed in the legend.

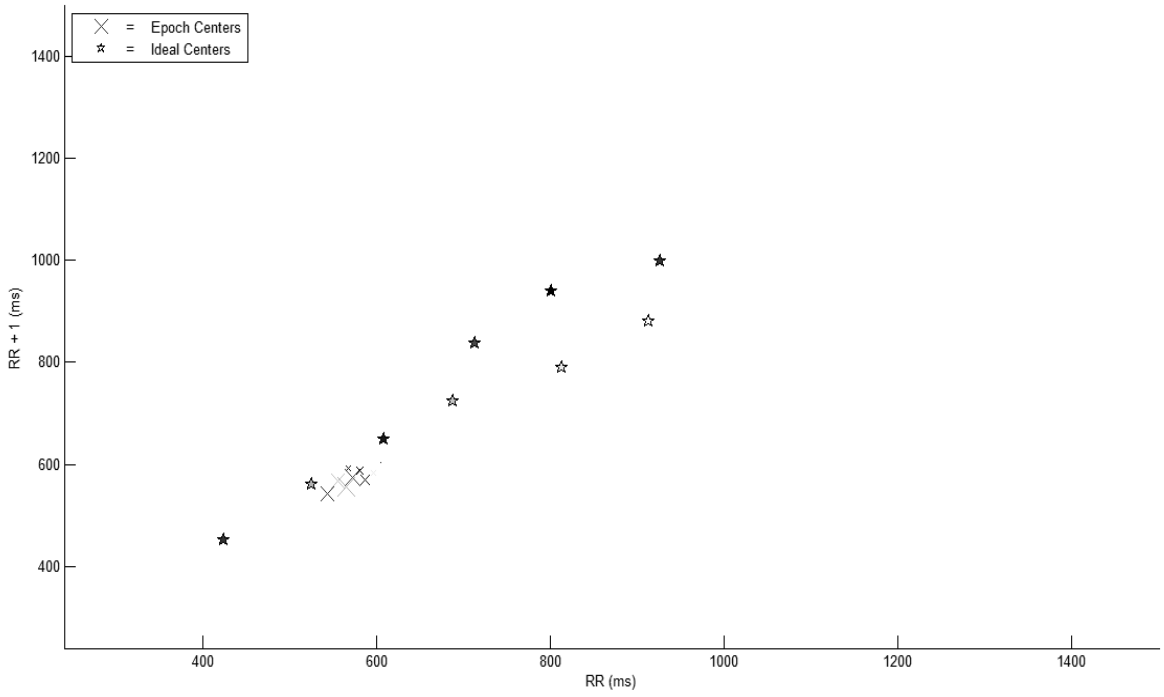

Figure 13. Plot of centers for first epoch of patient 1 with ideal centers superimposed.

For each of the two statistics described above, a threshold is set to indicate mortality. The thresholds were determined empirically, and each study patient was categorized as either live or die based on the last 2.5 hours of data obtained from each patient. The final 2.5 hours of the data was used for two reasons:

1. The record lengths for the patients varied depending on how long they were in the ICU.
2. With a perspective view, 2.5 hours contained enough data (5 points per statistic) to provide significant results.

Used to specify death, the empirically defined thresholds of 5000 and above for the mean and 1000 and above for the standard deviation were used on the CD data. MAD was also calculated for each epoch and an empirically defined threshold of 4.5 for the mean and above is used to specify death. The patients are analyzed into groups and the outcome is compared against the statistics. MAD provides a way to quantify disparate data in the presence of outliers, which is useful here due to measurement (patient moves inducing additional or missing heartbeat, etc.) and stochastic (heart rate suddenly increases due to loud sound, etc.) variations.

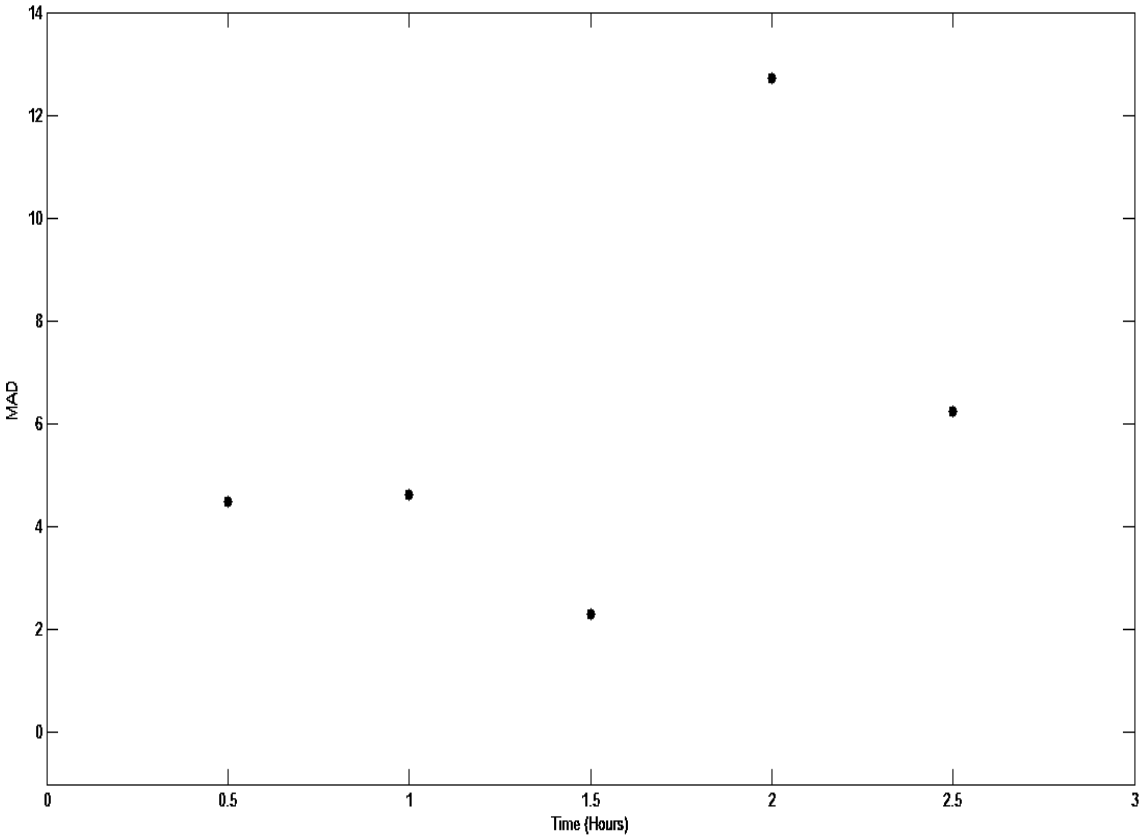

Figure 14. Plot of MAD for final 2.5 hours of data for patient 1.

CHAPTER 3

RESULTS AND DISCUSSION

AIM 1. For the first aim, inter-observer agreement is 96%, the same as found in the Woo study. The discordant observation is 1 patient who died. Both independent observers correctly classified:

1. Sensitivity = # True Positives/(# True Positives + # False Negatives) = 9/12 = 75%
2. Specificity = # True Negatives/(# True Negatives + # False Positives) = 9/12 = 75%
3. Positive Predictive Value (PPV) = # True Positives/(# True Positives + # False Positives) = 9/12 = 75%
4. Negative predictive Value (NPV) = # True Negative/(# True Negatives + # False Negatives) = 9/12 = 75%

Patient	Observer 1 Prediction	Observer 2 Prediction	Outcome
1	Die	Die	Die
2	Live	Live	Live
3	Live	Live	Live
4	Die	Die	Die
5	Live	Live	Live
6	Die	Die	Die
7	Die	Die	Die
8	Die	Die	Die
9	Die	Die	Live
10	Live	Live	Live
11	Live	Live	Live
12	Die	Die	Live
13	Live	Live	Live

Patient	Observer 1 Prediction	Observer 2 Prediction	Outcome
14	Live	Live	Live
15	Live	Live	Live
16	Die	Die	Die
17	Live	Live	Die
18	Die	Die	Die
19	Live	Live	Live
20	Die	Die	Die
21	Live	Die	Die
22	Live	Live	Die
23	Live	Live	Die
24	Die	Die	Live

Table 4. Chart of data collected for evaluation of Poincaré plots by the two trained observers.

Discharge status is predicted as alive if mostly Comet, and expired if mostly other shapes. Data contained herein shows that adult patient populations exhibit similar behavior and results to PICU patient populations. Some limitations of the current study include:

1. Retrospective study – not yet accomplished in real time to provide meaningful shifts in behavior on the part of the patient or doctor
2. Difficulty in assigning one predominant Poincaré shape to some subjects, especially since the shapes evolve and revolve over time
3. No specific exclusion criteria (though this can also be beneficial to proving the expanse of implications due to high sensitivity and specificity)
4. Unable to control for factors such as (though this can also be beneficial to proving the expanse of implications due to high sensitivity and specificity):
    a. Positive pressure ventilation
    b. Use of vasopressors and other hemodynamically significant drugs
    c. Patients' sleep/wake cycle

5. Unknown details of death (though this can also be beneficial to proving the expanse of implications due to high sensitivity and specificity):

AIM 2. Using two summary statistics, the sensitivity and specificity analysis of the reported outcome was calculated to evaluate the performance of the statistics and validate their clinical use. When studied independently, the cumulative distance statistic has a sensitivity of 100%, specificity of 33%, PPV of 60%, and NPV of 100%. The interpretation is that the algorithm is able to correctly identify 100% of the patients who are dying based on the previous 2.5 hours of heart rate variability and 33% of the patients who are not dying. Alternatively, the MAD has a sensitivity of 83%, specificity of 50%, PPV of 63%, and NPV of 75%.

Patient	Epoch 1 CD	Epoch 2 CD	Epoch 3 CD	Epoch 4 CD	Epoch 5 CD	Average / SD
2	4838.59	4812.36	4558.96	4840.12	4575.06	4725.0 / 144.8
3	4496.56	4759.63	4665.09	4626.60	4608.42	4631.3 / 95.3
5	3656.89	3135.74	3001.24	2864.15	2712.52	3074.1 / 361.8
9	3363.44	3496.22	5751.23	4717.90	3881.44	4242.0 / 995.3
10	3780.73	3850.68	3631.97	4016.50	3814.71	3818.9 / 138.3
11	4379.93	4405.49	4666.43	4290.88	4389.13	4426.4 / 141.4
12	3699.31	4463.04	5082.49	4081.06	3783.54	4221.9 / 566.5
13	3943.04	4184.14	4045.28	4502.87	4247.72	4184.6 / 213.9
14	3647.88	3914.33	3668.72	4007.99	3850.32	3817.8 / 156.2
15	4372.77	4636.11	4607.60	4594.12	4705.33	4583.2 / 125.2
19	4585.29	4660.24	4629.32	4556.18	4250.05	4536.2 / 164.9
24	1661.62	2934.20	1286.72	1372.06	1323.43	1715.6 / 697.1

Table 5. Cumulative Distance from Centers given for 5 ultimate epochs from surviving patients.

Patient	Epoch 1 CD	Epoch 2 CD	Epoch 3 CD	Epoch 4 CD	Epoch 5 CD	Average / SD
1	7464.71	10724.97	7403.97	10093.26	19577.72	11052.9 / 4997.3
4	3614.54	3341.37	4197.83	3736.41	4852.76	3948.6 / 592.7
6	3589.90	3572.24	3710.90	3415.52	7605.20	4378.8 / 1806.7
7	7372.65	1994.93	3345.76	3467.80	1469.08	3530.0 / 2313.4
8	2105.32	2086.34	2120.39	1625.60	2543.42	2096.22 / 324.9
16	6311.87	6282.43	5296.63	5001.88	3569.49	5292.5 / 1126.1
17	2542.69	2449.64	2549.51	2541.64	2511.27	2518.9 / 41.5
18	3335.24	3047.19	4154.20	4310.36	4698.17	3909.0 / 692.1
20	2927.04	3069.06	3096.40	3167.27	2723.94	2996.7 / 175.7
21	2388.62	2151.81	3004.07	2174.23	2928.29	2529.4 / 410.2
22	4859.37	4209.18	5277.52	3790.36	4286.12	4484.5 / 584.5
23	3926.95	3847.23	5404.62	4047.39	3827.32	4210.7 / 673.0

Table 6. Cumulative Distance from Centers given for 5 ultimate epochs from expiring patients.

Patient	Epoch 1 MAD	Epoch 2 MAD	Epoch 3 MAD	Epoch 4 MAD	Epoch 5 MAD	Average
2	0.05	2.04	0.05	0.05	2.09	0.85
3	1.69	1.69	1.69	1.69	8.77	3.11
5	4.62	1.05	0.94	0.93	1.76	1.86
9	7.25	9.54	19.13	4.36	2.85	8.63
10	4.49	3.03	3.10	3.00	2.88	3.30
11	2.09	4.03	3.89	9.64	2.14	4.36

Patient	Epoch 1 MAD	Epoch 2 MAD	Epoch 3 MAD	Epoch 4 MAD	Epoch 5 MAD	Average
12	1.34	5.00	7.52	3.03	4.33	4.25
13	1.52	1.55	1.52	3.80	0.04	1.68
14	2.85	1.42	2.85	1.37	2.85	2.27
15	0	0	0	0.04	1.95	0.40
19	1.99	1.90	1.90	3.89	5.31	3.00
24	6.99	9.53	3.79	4.52	5.48	6.06

Table 7. Median Absolute Deviation given for 5 ultimate epochs from surviving patients.

Patient	Epoch 1 MAD	Epoch 2 MAD	Epoch 3 MAD	Epoch 4 MAD	Epoch 5 MAD	Average
1	4.48	4.62	2.30	12.73	6.25	6.08
4	9.58	9.64	11.45	14.97	9.19	10.97
6	2.50	2.61	1.26	1.26	1.29	1.78
7	11.54	2.32	14.95	30.74	10.30	13.97
8	0.75	0.72	0.69	1.69	0.99	0.97
16	3.98	2.03	1.72	2.52	2.61	2.57
17	0	0	0	0.79	0.86	0.33
18	1.13	4.68	1.65	3.84	1.99	2.66
20	5.80	4.70	4.97	9.21	4.01	5.74
21	5.34	3.38	5.78	3.45	6.55	4.90
22	3.99	3.54	4.08	1.65	1.65	2.98
23	6.03	3.70	7.83	5.52	5.43	5.70

Table 8. Median Absolute Deviation given for 5 ultimate epochs from expiring patients.

Patient	Cumulative Distance Prediction	MAD Prediction	Outcome
1	Die	Die	Die
2	Live	Live	Live
3	Live	Live	Live
4	Live	Die	Die
5	Live	Live	Live
6	Die	Live	Die
7	Die	Die	Die
8	Live	Live	Die
9	Live	Die	Live
10	Live	Live	Live
11	Live	Live	Live
12	Live	Live	Live
13	Live	Live	Live
14	Live	Live	Live
15	Live	Live	Live
16	Die	Live	Die
17	Live	Live	Die
18	Live	Live	Die
19	Live	Live	Live
20	Live	Die	Die
21	Live	Die	Die
22	Live	Live	Die
23	Live	Die	Die
24	Live	Die	Live

Table 9. Chart of data collected for evaluation of Poincaré plots by the two summary statistics: CD and MAD.

However, when combined, using either a CD average greater than 5000, CD SD greater than 1000, or MAD average greater than 4.5, the sensitivity is 83%, the specificity is 67%, PPV is 71%, and NPV is 80%. In practice, it would be best to use the

cumulative distance independently to determine if a patient is dying and to use the combined statistics in order to determine if a patient is not dying.

Patient	Combined Prediction	Outcome
1	Die	Die
2	Live	Live
3	Live	Live
4	Die	Die
5	Live	Live
6	Die	Die
7	Die	Die
8	Live	Die
9	Die	Live
10	Live	Live
11	Live	Live
12	Live	Live
13	Live	Live
14	Live	Live
15	Live	Live
16	Die	Die
17	Live	Die
18	Live	Die
19	Live	Live
20	Die	Die
21	Die	Die
22	Live	Die
23	Die	Die
24	Die	Live

Table 10. Chart of data collected for evaluation of Poincaré plots by the combined summary statistic.

The second aim arises from the problem regarding Poincaré plot use having a lack of obvious quantitative measures that characterize the salient features of the plot.

The purpose for creating these statistics is to move in the direction of automating the mortality diagnosis and to remove observer biases.

A limitation to using the statistics as given is that the study has a limited number of patients and across a larger sample size, the statistics will not hold up as well. However, under the conditions given, there is much promise in using these two summary statistics to provide a real time response decision for patients who are most in need of attention.

CHAPTER 4

INNOVATION AND NOVELTY

AIM 1. The results derived from the first aim proved the clinical model. To date, Poincaré plots are only used in the laboratory setting and the ability to train healthcare professionals on the interpretation is now shown to be a legitimate method of prognoses in vivo. The data also represents the first use of Poincaré analysis for predicting survival in critically ill children. Different from previous studies, Poincaré plots are generated over a shorter duration (thirty minute epoch), whereas previously plots are created over a twenty-four hour time period. Therefore, the information contained in thirty-minute epochs maintained the integrity from which to derive valid conclusions by both replicating the observations of Woo and presenting statistically significant metrics. Since the plots are generated over a shorter duration, a "real time" assessment can be made on the data so that prompt interventions can be given as well as observation of the consequences of those interventions.

AIM 2. Cluster analysis is used to highlight where most data lie in Poincaré plots. A number of techniques have been tested in order to characterize the shape and underlying information contained within the Poincaré plot yet have had very limited success. Most are analogs to first dimensional statistical analyses on the heart rate variability data itself without using the Poincaré plot as a non-linear analysis technique. Now, with the creation of the cumulative distance statistic, the Poincaré plot can be exploited in a way not yet described. The MAD creates a statistic that is useful in data collected in the real world where model assumptions as well as data collection errors cannot be exactly controlled.

CHAPTER 5

CLINICAL IMPLICATIONS

HRV is a noninvasive measure of the balance of autonomic control on the heart, which has prognostic implications in health and human disease. From a clinical perspective, the ability to predict clinical outcomes (survival vs. death) in critically ill children, or more broadly, hospitalized patients helps guide clinical decision making and potentially, as an important input in end of life decision making (DNR: do not resuscitate status). Outside of the hospital, HRV metrics have the potential to facilitate triage care in disaster situations or on the battlefield during wartime or to assist in ambulatory care at home.

When physicians have reliable prognostic information, appropriate interventions can be utilized to improve the patient's clinical course and return them to health. Visual assessment of Poincaré plots generated during hospitalization in the PICU accurately predict patient outcome in approximately 75% of both pediatric survivors and deaths. Poincaré plots might be a very useful visual tool for bedside risk of mortality assessment by physicians and nurses. Additionally, it may be an important new input variable in a multivariate clinical decision support system for critically ill and hospitalized patients.

Heart rate Variability can be used to discover hidden health problems. If the nervous system is not controlling the body well, then anything can go wrong. A malfunctioning nervous system leads to a malfunctioning body. Since the nervous system controls sympathetic and parasympathetic activity, any health problem can affect its activity. Poincaré plots provide non-invasive prognoses into HRV and thus give healthcare professionals the ability to provide appropriate timely innervation.

Poincaré plots provide clinical insight into the workings of the nervous system. For this reason, Poincaré plots can be used to study a variety of health conditions instead of only cardiac disease. Poincaré plots provide a useful visual tool for bedside risk of mortality assessment. Poincaré plots are useful irrespective of pathology. If physicians have reliable prognostic information, then hopefully interventions are possible to change the patient's course!

CHAPTER 6

CONCLUSIONS AND FUTURE WORK

Poincaré plots are a semi-quantitative visual tool applied to the analysis of RR interval data resulting in a highly predictive assessment of survival in critically ill children. It allows for a simple and easily implemented method for the assessment of data that can be used in a clinical setting to augment current patient monitoring devices in providing “real time” visualization of heart rate variability data.

Poincaré plots detect patterns resulting from nonlinear processes that may not be observable by other methods of analysis. Other types of analysis provide summary evaluations of variation in RR intervals. Poincaré plots provide a beat-to-beat visual display that can reveal patterns resulting from nonlinear processes and non-periodic fluctuations.

Prior to Poincaré plot analysis, normal or CHF patients could be diagnosed based on SD (greater SD for normal patients), but could not predict mortality. SD is higher for normal Comet pattern than other types of patterns. There is no statistical difference for SD between the different unhealthy types of Poincaré patterns. Nor is there statistical significance for mortality based on the different unhealthy Poincaré patterns.

Additional variants of cluster analyses could be undertaken. These analyses can use simple statistical or geometrical parameters commonly used. Examples of such metrics as:

1. Densities – Number of data points associated with certain clusters.
2. Locations – Where the clusters are located both singularly and relative to other clusters.
3. Ratios – This can be a ratio of densities, locations, size, etc.
4. Extrema – Distances from furthest clusters.

5. Trajectory of cluster centers – Are the clusters contracting, expanding, or shifting?
6. Number of clusters 9 vs. ? – Using a different number of clusters may lead to more significant statistics.
7. Coupling with other types of real time continuously updated physiologic patient data such as oxygen saturation, respiratory rate, blood pressure, etc.
8. Combining Poincaré analyses with existing multivariate predictive analytics may yield more sensitive, specific and reliable real time predictions of patient outcomes.

Conducting a prospective validation study with larger patient population while acquiring other important patient and hospital outcomes data (i.e. impact on clinical decision making, correlation with healthcare providers assessments, length of stay, etc., would further the impact of the results stated herein.

REFERENCES

1. Akselrod S, Gordon D, Ubel FA, Shannon DC. Patterns of beat-to-beat heart rate variability in advanced heart failure. Science 1981;213:220-222.

2. Manzano BM, Vanderlei LC, Ramos EM, Ramos D.
Acute effects of smoking on autonomic modulation: analysis by Poincaré plot. Arq Bras Cardiol. 2011 Feb;96(2):154-60. Epub 2011 Jan 28.

3. Toichi M, Sugiura T, Murai T, Sengoku A. A new method of assessing cardiac autonomic function and its comparison with spectral analysis and coefficient of variation of R-R interval. J Auton Nerv Syst. 1997 Jan 12;62(1-2):79-84.

4. Porter TR, Eckberg DL, Fritsch JM, Rea RF, Beightol LA, Schmedtje JF Jr, Mohanty PK. Autonomic Pathophysiology in Heart Failure Patients. J Clin Invest. 1990 May;85(5):1362-71.

5. Cohn JN. Abnormalities of peripheral sympathetic nervous system control in congestive heart failure. Circulation 1990;82(suppl 1):I59-67.

6. Kleiger RE, Miller JP, Bigger JT, Moss AJ. Decreased Heart Rate Variability and Its Association with Increased Mortality After Acute Myocardial Infarction. Am J Cardiol 1987;59:256-62.

7. Redwood SR, Odemuyiwa O, Hnatkova K, Staunton A, Poloniecki I, Camm AJ, Malik M. Selection of dichotomy limits for multifactorial prediction of arrhythmic events and mortality in survivors of acute myocardial infarction. Eur Heart J. 1997 Aug;18(8):1278-87.

8. Stein PK, Domitrovich PP, Hui N, Rautaharju P, Gottdiener J. Sometimes higher heart rate variability is not better heart rate variability results of graphical and nonlinear analyses. J Cardiovasc Electrophysiol. 2005 Sep;16(9):954-9.

9. Pollack MM, Patel KM, Ruttimann UE. PRISM III an updated Pediatric Risk of Mortality score. Crit Care Med. 1996 May;24(5):743-52.

10. Woo MA, Stevenson WG, Moser DK, Trelease RB, Harper RM. Patterns of beat-to-beat heart rate variability in advanced heart failure. Am Heart J 1992;123:704-710.

11. Brown TE, Beightol LA, Koh J, Eckberg DL. Important influence of respiration on human R-R interval power spectra is largely ignored. J Appl Physiol. 1993 Nov;75(5):2310-7.

12. Guzik P, Piskorski J, Krauze T, Schneider R, Wesseling KH, Wykretowicz A, Wysocki H. Correlations between the Poincaré Plot and Conventional Heart

Rate Variability Parameters Assessed during Paced Breathing. J Physiol Sci. 2007 Feb;57(1):63-71. Epub 2007 Feb 3.

13. Heitmann A, Huebner T, Schroeder R, Perz S, Voss A. Multivariate short-term heart rate variability a pre-diagnostic tool for screening heart disease. Med Biol Eng Comput. 2011 Jan;49(1):41-50. Epub 2010 Dec 8.

14. Gladuli A, Moïse NS, Hemsley SA, Otani NF. Poincaré plots and tachograms reveal beat patterning in sick sinus syndrome with supraventricular tachycardia and varying AV nodal block. J Vet Cardiol. 2011 Mar;13(1):63-70. Epub 2011 Feb 1.

15. Huikuri HV, Seppänen T, Koistinen MJ, Airaksinen J, Ikäheimo MJ, Castellanos A, Myerburg RJ. Abnormalities in beat-to-beat dynamics of heart rate before the spontaneous onset of life-threatening ventricular tachyarrhythmias in patients with prior myocardial infarction. Circulation. 1996 May 15;93(10):1836-44.

16. Akselrod S, Gordon D, Ubel FA, Shannon DC, Berger AC, Cohen RJ. Power spectrum analysis of heart rate fluctuation: a quantitative probe of beat-to-beat cardiovascular control. Science. 1981 Jul 10;213(4504):220-2.

17. Kaplan EL, Meier P. Nonparametric estimation from incomplete observations. J. Amer. Statist. Assn. 1958;53:457–481.

18. Task Force of the European Society of Cardiology the North American Society of Pacing Electrophysiology. Heart Rate Variability: Standards of Measurement, Physiological Interpretation, and Clinical Use. Eur Heart J. 1996 Mar;17(3):354-81.

19. DT Kaplan. The Analysis of Variability. J Cardiovasc Electrophysiol. 1994;5:16-19.

20. Brennan M, Palaniswami M, Kamen P. Do Existing Measures of Poincaré Plot Geometry Reflect Nonlinear Features of Heart Rate Variability? IEEE Trans Biomed Eng. 2001 Nov;48(11):1342-7.

21. Tulppo MP, Mäkikallio TH, Takala TE, Seppänen T, Huikuri HV. Quantitative beat-to-beat analysis of heart rate dynamics during exercise. Am J Physiol. 1996 Jul;271(1 Pt 2):H244-52.

22. Marciano F, Migaux ML, Acanfora D, Furgi G, Rengo F. Quantification of Poincaré' maps for the evaluation of heart rate variability. Computers in Cardiology. 1994; 577-580.

23. Karmakar CK, Gubbi J, Khandoker AH, Palaniswami M. Analyzing temporal variability of standard descriptors of Poincaré plots. J Electrocardiol. 2010 Nov-Dec;43(6):719-24.

24. Esperer HD, Oehler M. Automatic quantification of the Poincaré plot asymmetry of NN-interval recordings. Physiol Meas. 2010 Mar;31(3):395-413. Epub 2010 Feb 10.

25. Karmakar CK, Khandoker AH, Gubbi J, Palaniswami M. Complex correlation measure a novel descriptor for Poincaré plot. Biomed Eng Online. 2009 Aug 13;8:17.

26. Karmakar CK, Khandoker AH, Gubbi J, Palaniswami M. Defining asymmetry in heart rate variability signals using a Poincaré plot. Physiol Meas. 2009 Nov;30(11):1227-40. Epub 2009 Oct 8.

27. Mohan A, James F, Fazil S, Joseph PK. Design and Development of a Heart Rate Variability Analyzer. J Med Syst. 2012 Jun;36(3):1365-71. Epub 2010 Nov 6.

28. Piskorski J, Guzik P. Geometry of the Poincaré plot of RR intervals and its asymmetry in healthy adults. Physiol Meas. 2007 Mar;28(3):287-300. Epub 2007 Feb 19.

29. Maestri R, Pinna GD, Accardo A, Allegrini P, Balocchi R, D'Addio G, Ferrario M, Menicucci D, Porta A, Sassi R, Signorini MG, La Rovere MT, Cerutti S. Nonlinear indices of heart rate variability in chronic heart failure patients redundancy and comparative clinical value. J Cardiovasc Electrophysiol. 2007 Apr;18(4):425-33. Epub 2007 Jan 30.

30. Stein PK, Domitrovich PP, Huikuri HV, Kleiger RE; Cast Investigators. Traditional and nonlinear heart rate variability are each independently associated with mortality after myocardial infarction. J Cardiovasc Electrophysiol. 2005 Jan;16(1):13-20.

31. Zemaityte D, Varoneckas G, Ozeraitis E, Podlipskyte A, Valyte G, Zakarevicius L. Heart Rate Poincaré Plots and Their Hemodynamic Correlates: Discrimination Between Sinus and Ectopic Rhythms. Biomedicine. 2001;1(2):80–89.

32. Ng, H.P., Ong, S.H., Foong, K.W.C., Goh, P.S., Nowinski, W.L., "Medical Image Segmentation Using K-Means Clustering and Improved Watershed Algorithm", Image Analysis and Interpretation, 2006 IEEE Southwest Symposium on, On page(s): 61 - 65

33. T. Kanungo, D. M. Mount, N. Netanyahu, C. Piatko, R. Silverman, & A. Y. Wu (2002) An efficient k-means clustering algorithm: Analysis and implementation Proc. IEEE Conf. Computer Vision and Pattern Recognition, pp.881-892.

34. Li-Hong Juang, Ming-Ni Wu, Psoriasis image identification using k-means clustering with morphological processing, Measurement, Volume 44, Issue 5, June 2011, Pages 895-905

35. S. Sahiner, H.-P. Chan, and N. Petrick et al., "Computerized characterization of masses on mammograms: the rubber band straightening transform and texture analysis", Med. Phy. Vol.25(4), 1998, pp.516-526.

36. E.A. Hoffman, J.M. Reinhardt, and M. Sonka et. al, "Characterization of the interstitial lung diseases via density-based and texture-based analysis of computed tomography images of lung structure and function", Acad. Radiol. Vol. 10(10), 2003, pp.1104-1118.

37. Niskanen JP, Tarvainen MP, Ranta-Aho PO, Karjalainen PA. Software for advanced HRV analysis. Comput Methods Programs Biomed. 2004 Oct;76(1):73-81.

38. Kim KK, Baek HJ, Lim YG, Park KS. Effect of missing RR-interval data on nonlinear heart rate variability analysis. Comput Methods Programs Biomed. 2012 Jun;106(3):210-8. Epub 2010 Dec 30.

39. Maestri R, Pinna GD, Porta A, Balocchi R, Sassi R, Signorini MG, Dudziak M, Raczak G. Assessing nonlinear properties of heart rate variability from short-term recordings are these measurements reliable. Physiol Meas. 2007 Sep;28(9):1067-77. Epub 2007 Aug 21.